Journal of Magnetic Resonance 203 (2010) 73–80

Contents lists available at ScienceDirect

Journal of Magnetic Resonance

journal homepage: www.elsevier.com/locate/jmr

Selective heteronuclear Hartmann–Hahn: A multiple-pulse sequence for selective magnetization transfer in the structural elucidation of "isotagged" oligosaccharides

Xi Meng [1], William H. Nguyen, James S. Nowick, A.J. Shaka *

Department of Chemistry, University of California, Irvine, CA 92697-2025, USA

ARTICLE INFO

Article history:
Received 4 August 2009
Revised 2 December 2009
Available online 30 December 2009

Keywords:
2D NMR
Heteronuclear Hartmann–Hahn
Polarization transfer
Peracetylation
Selective
Glycan
Oligosaccharide
Scandium triflate

ABSTRACT

A new selective heteronuclear Hartmann–Hahn (SHEHAHA) multiple-pulse mixing sequence is proposed for the solution structure elucidation of milligram amounts of peracetylated oligosaccharides in which the acetyl groups are enriched in carbon-13, so-called "isotags". SHEHAHA accomplishes exclusive in-phase magnetization transfer between the isotag carbonyl ^{13}C and the proximal proton on the sugar ring. Relayed transfer around the sugar rings by proton–proton TOCSY is suppressed, while the heteronuclear transfer from the labeled carbonyl carbon to the proximal ring proton is maintained. The sequence is broadband in the sense that all acetyl groups simultaneously give good signal transfer to their respective nearest proton neighbors. The ^{1}H-detected spectra have decent sensitivity and excellent resolution, giving patterns that unambiguously identify common structural subunits in human glycans. Peracetylated maltitol is shown as a test case of the method. Lineshapes are pure absorption, allowing facile measurement of vicinal proton–proton couplings. Linkage points can be deduced, and the 2D correlation spectra may be useful for more ambitious prediction algorithms and machine identification by a spectral database.

© 2009 Elsevier Inc. All rights reserved.

1. Introduction

Double resonance in the rotating frame, described by Hartmann and Hahn in 1962 [1], and commonly known as "cross polarization" today, is routinely used in solid-state NMR to improve the sensitivity of dilute low-γ spins that are dipolar coupled to abundant high-γ spins, the most common application being ^{13}C enhancement by ^{1}H [2]. With the advent of broadband multiple-pulse mixing sequences, cross polarization was extended to liquid-state NMR, where magnetization transfer relies on the much smaller scalar J coupling [3–8]. Compared to application of a conventional continuous wave (CW) radiofrequency (rf) magnetic field B_1, these multiple-pulse mixing sequences show less sensitivity to off-resonance effects and the influence of the latter on the Hartmann–Hahn matching condition

$$\gamma_I B_{1_{I_{eff}}} = \gamma_S B_{1_{S_{eff}}} \quad (1)$$

in which the effective field $B_{1_{eff}}$ includes the resonance offset; the attainable magnetization transfer yield is only high when $|\gamma_I B_{1_{I_{eff}}} - \gamma_S B_{1_{S_{eff}}}| < |J|$ and when the effective fields have a large transverse component in the CW case. Departure from this fairly stringent matching condition leads to poor magnetization transfer and hence poor sensitivity in a 2D spectrum using this mode of transfer. Employing synchronized multiple-pulse sequences on both I and S shows much better tolerance for resonance offset, although it is still not currently possible to obtain efficient cross polarization over the entire protonated ^{13}C (160 ppm) bandwidth at high field using attainable rf power and current liquid probe technology. The moniker heteronuclear Hartmann–Hahn (HEHAHA) is often used in the liquids literature, to distinguish the experiment from the more common TOCSY [9] experiment, known briefly as homonuclear Hartmann–Hahn (HOHAHA). As the Hartmann–Hahn experiment originally applied to the heteronuclear case, "HEHAHA" is slightly redundant. Nevertheless, for continuity with the literature, we will continue to use this designation. Our selective HEHAHA sequence will be denoted SHEHAHA. In addition, our magnetization transfer pathway is from ^{13}C to ^{1}H and both are at *ca.* 100% abundance. As magnetization is transferred in both directions by HEHAHA, we did not choose to label the sequence as reverse HEHAHA even though the traditional roles of the two spin species are reversed here.

The multiple-pulse HEHAHA sequences also foster *homonuclear* magnetization transfer, TOCSY. In the present case, TOCSY among the ^{13}C spins is not a concern. Indeed, broadband carbon-13 TOCSY remains an unsolved problem at high field. Carbon-13 TOCSY was

* Corresponding author. Fax: +1 949 824 9920.
E-mail address: ajshaka@uci.edu (A.J. Shaka).
[1] Present address: Varian China Beijing Office, 1648 Central Tower South Wing, Beijing Junefield Plaza, No. 10 XuanWuMenWai Street, Beijing 100052, PR China.

1090-7807/$ - see front matter © 2009 Elsevier Inc. All rights reserved.
doi:10.1016/j.jmr.2009.12.003

demonstrated over the full ^{13}C bandwidth with the FLOPSY sequence [10], but only at 7 T magnetic field strength, where the protonated ^{13}C chemical shift range is 12 kHz. However, proton TOCSY is easier to do. In particular, magnetization transfer through long-range $^{n}J_{CH}$ couplings, in which sufficient rf power may need to be applied to both sets of spins, will apparently always result in parasitic TOCSY among the protons themselves. If total correlation is the aim, as it is in TOCSY, this transfer is welcome. If, however, a definitive assignment of a particular peak in a 2D spectrum to a particular coupled CH pair is the aim, the additional relayed transfer to other protons that are not necessarily coupled to the carbon-13 peak of interest, is unwanted. While this effect can be limited by reducing the field strength of multiple-pulse mixing sequences [11,12] or by using selective pulses in the multiple-pulse mixing sequences [13,14], the heteronuclear Hartmann–Hahn transfer is still typically band-selective. As the $^{1}H_{Ring}$ protons in peracetylated oligosaccharides fall within a band, TOCSY among them is to be expected. The SHEHAHA mixing sequence proposed in this work takes advantage of the particular characteristics of isotagged sugars to give selective magnetization transfer from each isotag carbonyl to its respective proximal ring proton, while largely suppressing the homonuclear Hartmann–Hahn transfer. In a certain sense, the innovation is mostly to abandon more elaborate mixing sequences, and return to the simpler scheme of Hartmann and Hahn, albeit with a few important adjustments.

SHEHAHA was motivated by both the successful application of more conventional DIPSI-2 based HEHAHA in the structure elucidation of oligosaccharides in which the free hydroxyl groups are esterified with doubly ^{13}C-labeled acetyl groups [15–17] and simultaneous frustration with some aspects of the spectra obtained, particularly with respect to copies of peaks across multiple traces. This "striping" of peaks adds to spectral congestion and lowers the achievable resolution. In the existing pulse sequences for peracetylated oligosaccharides [15] during the key acetyl $^{13}CO \rightarrow {}^{1}H_{Ring}$ magnetization transfer step, synchronous matched DIPSI-2 sequences transfer magnetization by means of the small 2–5 Hz $^{3}J_{CH}$ couplings. In practice, mixing times τ of 200 ms or more may need to be employed to get optimum magnetization transfer. However, during this long mixing time, both heteronuclear and homonuclear Hartmann–Hahn transfers are effected by the DIPSI-2 mixing sequence which is, of course, highly efficient for proton–proton TOCSY [8]. Each acetyl ^{13}CO isotag thus shows a stripe of correlations with many ring protons in the same sugar ring, as a result of the simultaneously occurring heteronuclear and homonuclear magnetization transfers. This relayed transfer is a strength, as it allows the identification of separate spin systems, but it is also a weakness, as it is not a simple matter to determine which particular proton multiplet in the stripe derives from the proximal proton to the tag. Furthermore, sensitivity is reduced when the available source reservoir of ^{13}CO magnetization is distributed over a larger number of destination peaks, and the spectra can be somewhat cluttered when the protons from distinct rings happen to have degenerate chemical shifts. By its selective nature, SHEHAHA is able to minimize extraneous acetyl ^{13}CO–$^{1}H_{Ring}$ correlation peaks by suppressing the TOCSY transfer. This makes the assignment easier, while still allowing a separate correlation of the protons amongst themselves, in an added dimension of a higher-dimensional experiment, if desired. While a simple INEPT [18] transfer with quite long delays could also give just the correlation to the proximal proton, the small antiphase splitting superimposed on complex proton multiplets results in antiphase multiplet patterns if carbon-13 decoupling is not used. An additional rephasing delay, to avoid the antiphase problem and allow ^{13}C carbonyl decoupling, is unfortunately long compared with $1/J_{HH}$ for typical proton couplings, resulting in phase-modulated multiplets, rather like those observed in HMBC [19] experiments from which the vicinal J_{HH} values can be extracted only with some difficulty. As the stereochemical analysis of each sugar ring is based on the numerical values of the vicinal couplings, the more familiar pure *in-phase* multiplet patterns from the Hartmann–Hahn transfer are much preferred.

The doubly ^{13}C-labeled acetyl derivatives are known [15,16] to have the following advantages for NMR-based oligosaccharide structure elucidation: (i) improved proton spectral dispersion caused by the electron withdrawing acetyl groups; (ii) flexibility in design and development of multi-dimensional NMR pulse sequences, facilitated by well separated acetyl $^{1}H_{Me}$, $^{13}C_{Me}$, ^{13}CO and $^{1}H_{Ring}$ frequency dimensions; and (iii) the possibility to prepare quite concentrated solutions in organic solvents like $CDCl_3$ to take advantage of smaller, more sensitive NMR probes when the absolute amount of material is marginal. Condensing a high-resolution 4D experiment [17] to a 2D experiment, in conjunction with a simplified synthesis of the derivatives makes the method more rapid and practical to employ.

2. Theory

Analysis of homonuclear Hartmann–Hahn (TOCSY) experiments is available in the literature [9,20], as is the heteronuclear version [21–23], and will not be recapitulated in detail here. Briefly, under a suitably-designed multiple-pulse sequence, or strong CW irradiation along the *x*-axis in the rotating frame for both proton and carbon channels for a time τ, the average Hamiltonian [24] for heteronuclear magnetization transfer, to zeroth-order, is

$$\overline{\mathscr{H}}_{IS} = 2\pi\frac{J_{IS}}{2}(I_yS_y + I_zS_z) \tag{2}$$

while that for the homonuclear case is

$$\overline{\mathscr{H}}_{II} = 2\pi J_{II}(I_{1x}I_{2x} + I_{1y}I_{2y} + I_{1z}I_{2z}). \tag{3}$$

Under these average Hamiltonians, in-phase magnetization transfer is obtained from $S_x \rightarrow I_x$ and $I_{1x} \rightarrow I_{2x}$, respectively, as follows:

$$S_x \overset{\tau\overline{\mathscr{H}}_{IS}}{\rightarrow} \frac{S_x + I_x}{2} + \frac{S_x - I_x}{2} cos\pi J_{IS}\tau - (I_yS_z + I_zS_y)sin\pi J_{IS}\tau \tag{4}$$

and

$$I_{1x} \overset{\tau\overline{\mathscr{H}}_{II}}{\rightarrow} \frac{I_{1x} + I_{2x}}{2} + \frac{I_{1x} - I_{2x}}{2} cos2\pi J_{II}\tau + (I_{1y}I_{2z} - I_{1z}I_{2y})sin2\pi J_{II}\tau. \tag{5}$$

If strong enough irradiation is used on both ^{13}C and ^{1}H then both these transfers will occur, leading to the relay of magnetization $S_x \rightarrow I_{1x} \rightarrow I_{2x}$ in sugar spin systems. As the long-range $^{3}J_{CH}$ coupling from the carbonyl carbon is much smaller than many $^{3}J_{HH}$ couplings, and there is a factor of two reduction in efficiency for heteronuclear magnetization transfer, magnetization represented by I_{1x} arriving at the proximal ring proton is rapidly redistributed along the coupling network. The transfer functions become complex [25,26] and, as the couplings have unknown values, it is not possible to choose τ to limit or edit the relayed peaks in a useful way.

Instead, we exploit the particular NMR spectral properties of these acetylated sugars to achieve selectivity. Briefly, the acetyl carbonyl chemical shift range is within 2 ppm or 250 Hz at 125 MHz for ^{13}C, the ^{1}H chemical shift range of the ring protons is 2-3 ppm, and the three-bond acetyl ^{13}CO–$^{1}H_{Ring}$ couplings are (2–5 Hz) in the peracetylated oligosaccharides we have studied. The very limited carbonyl chemical shift range is a boon, as is the extremely narrow (< 0.5 Hz) carbonyl line width. Under these conditions, a relatively low-power CW irradiation 1.0–1.5 kHz may be enough to dominate the chemical shift range on both ^{13}C and ^{1}H, and a fairly long duration τ can be used without fearing damage to the probe circuitry. It is well known that weak CW irradiation leads to a very poor Hartmann–Hahn match, and hence very

limited TOCSY magnetization transfer, when the carrier frequency is placed to one side of the spectral range, a fact that has been exploited in various versions of the CW ROESY experiment [27,28] in which rotating-frame cross-relaxation peaks are desired but relayed magnetization transfer is certainly not. In SHEHAHA the proton transmitter is set to slightly low- or high-frequency of the known $^1H_{Ring}$ proton chemical shift range. For a 5 Hz $^3J_{CH}$ coupling, the maximum offset from the proton transmitter frequency over which HEHAHA magnetization transfer is efficient, for the case of simultaneous 1 kHz CW irradiation and where the carbon-13 transmitter is on resonance, is only about ±100 Hz. This 100 Hz is also the minimum chemical shift separation required between two coupled protons to avoid unwanted TOCSY, if the proton transmitter frequency were to be set at the resonance frequency of one of the two protons. At first glance, it seems unlikely to get efficient broadband C → H magnetization transfer for all the isotag sites. However, two factors enter in to improve the prospects of success. First, the doubly labeled acetyl groups have a 55 Hz $^1J_{CC}$ coupling, further split into 7 Hz $^2J_{H_{Me}C}$ quartets. As Fig. 1 shows, these extra couplings broaden the matching condition in the carbonyl region so that there are multiple possibilities to achieve a good match, and hence for efficient magnetization transfer. Of course, not all transitions will participate fully, so that sensitivity is reduced. However, without the relayed transfer, the available signal is not diluted by distribution to other proton spin multiplets. On balance, sensitivity of a typical 2D peak in the selective experiment is worse than that with synchronous DIPSI-2 irradiation by a variable factor of 5–10 depending on the details of the spin system, the amount of power used, and how carefully the match is optimized. While the sensitivity is mediocre, the selectivity is excellent. Secondly, once the proton transmitter is positioned even 50 Hz outside the $^1H_{Ring}$ chemical shift range, so that the frequencies with respect to the carrier become 50 and 150 Hz rather than 0 and 100 Hz, the two protons will give negligible TOCSY. Thus, offsetting the proton transmitter by just 0.1 ppm to either side of the ring proton range is sufficient to mismatch the TOCSY condition over the whole band. Exactly as in the elegant jump-symmetrized ROESY experiment [27], both the low- and high-frequency possibilities can be coalesced into a single sequence by frequency-hopping the proton transmitter, re-aligning the spin-locked magnetization by a suitable pulse or sequence of pulses, to avoid signal loss. This modified mixing sequence forms the heart of the SHEHAHA technique.

In the experiments shown here, the 5.5 ppm position was chosen first, and the duration of the first segment of the irradiation was 100 ms. During this time, the ring protons from 4.75 to 5.5 ppm approximately satisfy the Hartmann–Hahn condition, but the other protons do not. Accordingly, magnetization transfer proceeds to protons in about half of the total band, but not to any others. When the proton transmitter is switched to the opposite end of the band for a similar 100 ms irradiation, the 4.75–5.5 ppm band is mismatched, so that the magnetization there begins to decay with a time constant $T_{1\rho,off}$. Meanwhile the protons from 4.0 to 4.75 ppm are matched, and magnetization transfer proceeds to them. This piecemeal transfer of polarization allows fairly good net magnetization transfer across the entire chemical shift range. The weak rf field is appreciably tilted at the other edge of the band, but a short, hard $+y$-phase β-pulse is sufficient to realign the proton magnetization along the effective field and minimize losses after the frequency is switched; on the Varian UnityPlus spectrometer, the correct integer phase setting for this pulse is "3", rather than "1". The flip angle β is given by

$$\beta = tan^{-1}\left(\frac{2\pi\Delta f}{\gamma_I B_{1I}}\right) \tag{6}$$

for a frequency hop of Δf Hz.

3. Materials and methods

3.1. Acetylation procedure

A capped, oven-dried, 3-mL conical vial was charged with 0.0184 g (0.0533 mmol) of finely ground maltitol, and 0.0009 g

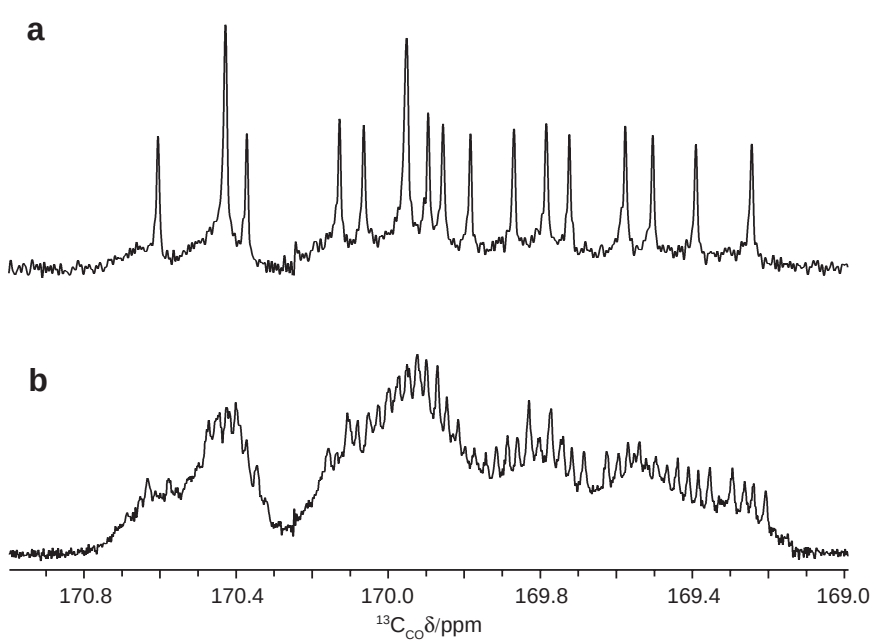

Fig. 1. Carbon-13 spectrum of peracetylated maltitol with doubly-labeled acetyl groups (a) with and (b) without decoupling of ^1H during acquisition. Only the acetyl ^{13}CO spectral region is shown. The large one-bond 55 Hz couplings in (a) originate from the methyl carbon, while the additional quartet structure in (b) results from the methyl protons. There are also small doublets from the $^1H_{Ring}$ couplings, but these are smaller than the splittings from the methyl groups. During SHEHAHA, the weak irradiation is insufficient to affect either the methyl carbons or methyl protons directly to any appreciable level, so that spectrum (b), with its multiple opportunities for effective Hartmann–Hahn matching, is the more correct picture to keep in mind to understand the dynamics of magnetization transfer.

(0.002 mmol) scandium triflate catalyst. A magnetic stirring vane and 0.141 mL (1.49 mmol) acetic anhydride-$^{13}C_4$, were added, the vial was capped, and the mixture was stirred at room temperature for 8.5 h. The majority of the acetic acid by-product and unreacted acetic anhydride liquids were removed by rotary evaporation. The remaining acetic acid and acetic anhydride were removed using a high vacuum for 1 h. to yield 0.03671 g (93%) of peracetylated maltitol as a clear, gummy solid.

This abbreviated synthetic method works well on a range of non-ionic oligosaccharides. The scandium triflate catalyst is particularly useful as Sc^{3+} has a d^0 electron configuration, and hence will not broaden the NMR lines if it is not entirely removed. Triflate has no proton NMR signal, making its presence likewise innocuous. This Lewis acid catalyst is well known in the synthetic chemistry literature [29] and proved to be the simplest way to conduct the peracetylation with expensive labeled reagents and at small scale. As is apparent from Fig. 1(a) the product seems to contain minor impurities that contribute to some apparent spectral line broadening, but which fortunately are not seen the 2D spectra.

3.2. Radiofrequency calibration

The rather long and weaker CW pulses used in SHEHAHA are best calibrated by using off-resonance carbon-13 decoupling of a simple molecule like chloroform, the usual solvent for the peracetylated sugars. A small amount of $CHCl_3$ in $CDCl_3$ is an adequate calibration standard. The carbon-13 satellites are easy to discern, and locating the exact position of the carbon-13 resonance by observing when the splitting is removed completely is straightforward. The carbon-13 frequency is then offset by about 100 Hz or so from exact resonance and the scaled splitting observed. The well-known scaling factor [30],

$$\lambda = \frac{J_r}{J} = \frac{\Delta f}{\sqrt{(\Delta f)^2 + (\gamma_C B_{1C}/2\pi)^2}} \tag{7}$$

where J_r is the observed reduced splitting under carbon-13 irradiation, and Δf is the frequency offset from resonance, can then be used to determine $\gamma_C B_{1C}/2\pi$. The reduced proton power can be obtained by finding the 360° pulse width on the center chloroform singlet. It is inaccurate to extrapolate the low-power settings from high-power pulse widths because the attenuation is not exactly linear over very wide dynamic range. Once the calibrations have been performed on the standard, they are stable on sequential samples as long as the probe tuning and matching can be optimized to the same reflected power.

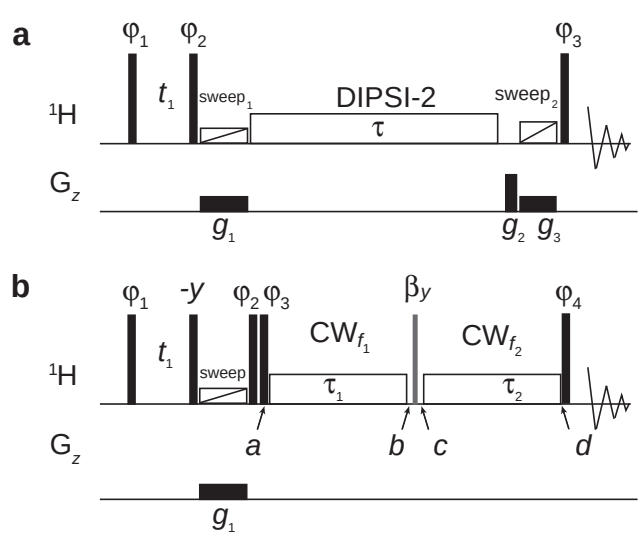

Fig. 2. Pulse sequences used to explore the presence or absence of proton magnetization transfer during the heteronuclear mixing sequence. (a) The timing diagram for *z*-filtered TOCSY using DIPSI-2 mixing. (b) The timing diagram for a test of the mixing sequence used in the SHEHAHA method (Fig. 5). Filled narrow rectangular icons represent hard 90° pulses. Frequency-swept inversion pulses for the *z*-filter are represented by open, scored, rectangular icons. The durations and strengths of the pulsed magnetic field gradients (rectangular) are $g_1 = (30\ \text{ms}, 0.89\ \text{G/cm})$, $g_2 = (100\ \mu\text{s}, 8.9\ \text{G/cm})$, $g_3 = (20\ \text{ms}, 0.89\text{G/cm})$. In (a), the phase cycle is $\varphi_1 =, (x, -x, -x, x), \varphi_2 = 2(x), 2(-x), \varphi_3 = x, Rx = 2(x, -x)$. In (b), $\varphi_1 = y, \varphi_2 = 2(x, , -y)$ $\varphi_3 = 2(x), 2(-x), \varphi_4 = 4(x), 4(-x), Rx = 2(x, -y)$. The flip angle of the β_y pulse in (b) depends on the frequency difference $f_1 - f_2$ as described in the text. Details of transmitter position, field strength, mixing time, *etc.* are found in the captions of Figs. 4 and 5.

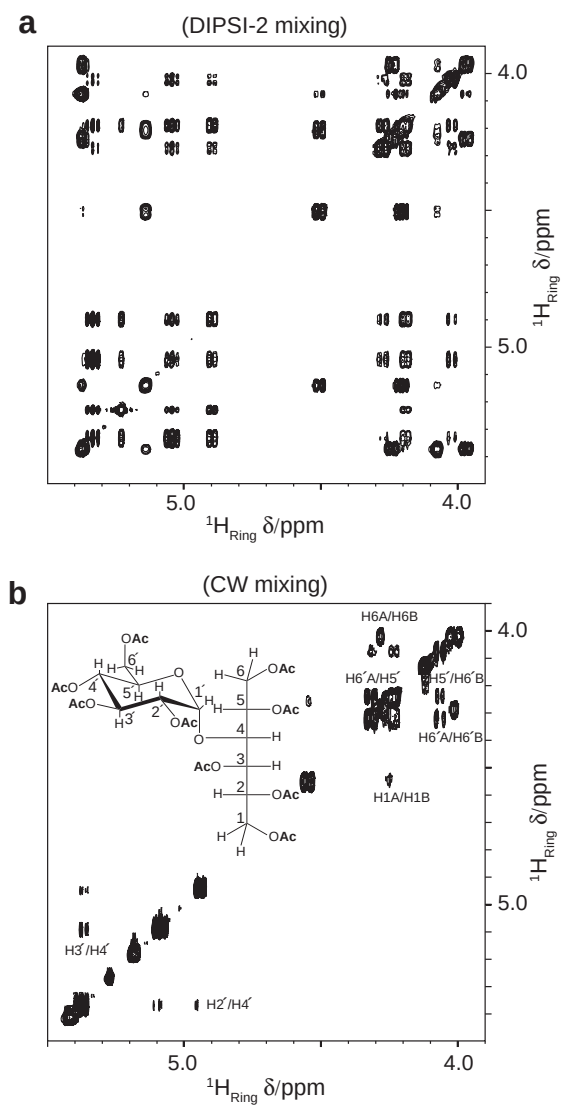

Fig. 3. Two-dimensional proton correlation spectra using the mixing sequences of Fig. 2(a) and Fig. 2(b). Data were acquired with 512 and 3300 complex data points over spectral widths of 3300 Hz in F_1 and F_2, respectively. The large number of TOCSY cross peaks resulting from DIPSI-2 mixing are pruned way down to just a few cross peaks using the time-shared CW mixing sequence in (b). Only coupled protons with quite close chemical shifts give any peaks at all, and the peaks are quite weak except for the case of geminal protons, where they are unimportant, as both geminal protons are proximate to the carbonyl isotag and help to identify the primary hydroxyl sites. Note, however, the cross peaks observed between H6′A and H5′, because of the nearly degenerate chemical shifts of these two protons.

4. Experimental

All 2D spectra were recorded at 25 °C and 500-MHz. A standard Varian UnityPlus spectrometer equipped with a conventional HCN triple-resonance probe with triax pulsed field gradients was used to record the proton spectra, while the 1D carbon spectra were recorded using a carbon-13 direct detect probe.

A 2D TOCSY experiment using the frequency-hopped mixing sequence employed for SHEHAHA serves to show the degree of TOCSY suppression that can be expected among the sugar ring protons. No appreciable proton magnetization is produced during the SHEHAHA mixing that is antiphase with respect to *proton* couplings, so the antiphase terms that naturally develop during t_1 in the TOCSY test sequence were purged using a frequency-swept 180° pulse while a strong *z*-gradient is maintained [31]. This was sandwiched between two 90° pulses before the mixing period and proved to be an excellent single-scan *z*-filter. Without removal of the antiphase proton magnetization, unwanted COSY cross peaks would occur, spoiling the TOCSY selectivity assessment. These irrelevant COSY peaks would not, however, occur in the SHEHAHA experiment itself. The pulse sequence timing diagram is shown in Fig. 2(b). Two *z*-filters were used to record the conventional TOCSY spectrum using DIPSI-2 (Fig. 2(a)) as DIPSI-2 itself generates zero-quantum coherence during the TOCSY transfer.

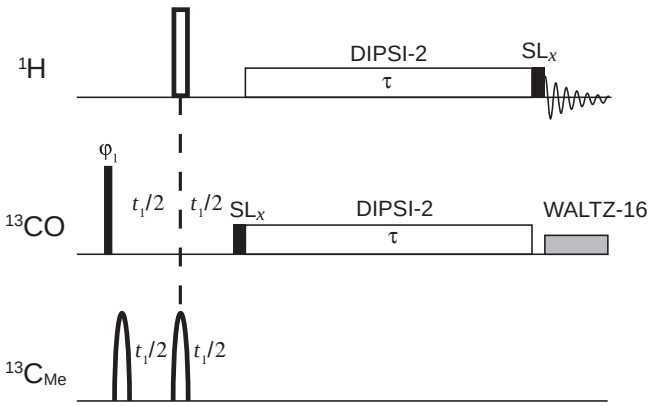

Fig. 4. Pulse sequence used to record the $^{13}CO-{}^1H_{Ring}$-HEHAHA spectrum. Wide open bar icons represent hard 180° pulses and narrow filled bars represent hard 90° pulses. Frequency-selective 180° pulses are represented as open curved icons. Decoupling of $^{13}C_{Me}$ during t_1 is achieved with a pair of phase-modulated selective pulses, each of duration 100 μs, that cleanly invert the $^{13}C_{Me}$ spins. Low-power WALTZ-16 is used to decouple ^{13}C during acquisition; only the carbonyl region is targeted. Quadrature detection in the ^{13}CO dimension is achieved with "States-TPPI" [32] phase cycling of φ_1. The ^{1}H transmitter is placed in the center of the ring proton region (4.7 ppm) and the ^{13}C transmitter centered in ^{13}CO region (170.0 ppm). Simultaneous DIPSI-2 mixing sequence with a field strength of 930 Hz applied for a period of 200 ms effects magnetization transfer. The phase cycle is $\varphi_1 = (y, -y)$, $Rx = (y, -y)$. A brief spin lock period of 10 ms was used to dephase unwanted magnetization, although it does not completely remove homonuclear zero-quantum coherence that DIPSI-2 may generate.

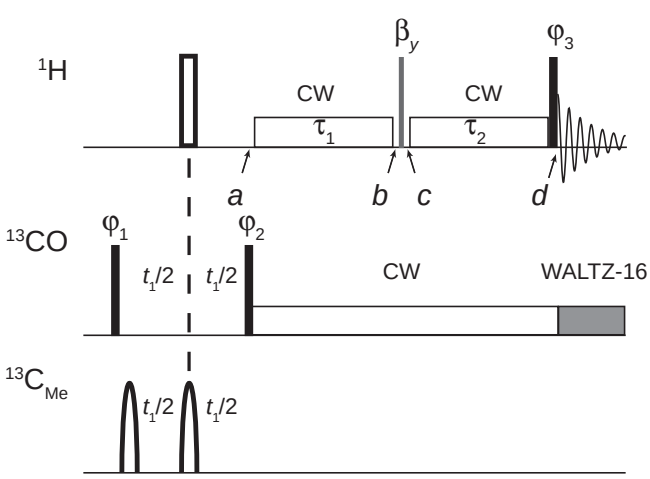

Fig. 5. Pulse sequence used to record the $^{13}CO–{}^1H_{Ring}$-SHEHAHA spectrum. Icons are as in Fig. 4.The ^{1}H transmitter is initially placed at the center of the ring protons (4.7 ppm) and the ^{13}C transmitter is kept at the center of the ^{13}CO region (170.0 ppm). Subsequently the ^{1}H transmitter is moved to the left side of the $^1H_{Ring}$ spectrum (5.5 ppm) at point a. At point b, the ^{1}H transmitter is moved back to the center, then moved to the right side of the $^1H_{Ring}$ spectrum (3.9 ppm) at point c. At point d the ^{1}H transmitter is moved back to the center again. Heteronuclear Hartmann–Hahn mixing uses a CW rf with a field strength of 930 Hz applied on both the proton transmitter for a period of 100 ms for both τ_1 and τ_2, and applied on the carbon transmitter for 200 ms. The phase cycle is $\varphi_1 = (y, -y), \varphi_2 = (x, x, -x, -x), \varphi_3 = 4(x), 4(-x), Rx = (y, -y)$.

Fig. 3 shows the comparison of the 2D spectra obtained with the two mixing sequences of Fig. 2, recorded on a peracetylated maltitol sample containing natural abundance carbon in the acetyl groups. In Fig. 3(b), the TOCSY peaks have been greatly suppressed, although some peaks close to the diagonal still arise. These small TOCSY peaks occur between non-equivalent geminal protons or between protons which have quite close resonance frequencies and large J-coupling. The first case presents no problem in the SHEHAHA spectrum, as both non-equivalent geminal protons would be expected to correlate with the proximal isotag. For the latter case, the homonuclear Hartmann–Hahn transfers between H3′ – H4′, *H*3′ – H2′, H5′ – H6′A and H5′ – H6′B are partially suppressed; they are barely observed in the acetyl $^{13}CO-{}^1H_{Ring}$ SHEHAHA spectrum. However, it is necessary to analyze the SHEHAHA spectrum carefully for peaks whose resonance frequencies may be similar. For instance, in Fig. 3(b), H5′ could be mistaken for a direct heteronuclear Hartmann–Hahn transfer to H6′B. Oftentimes a reciprocal transfer peak occurs, to give a square pattern that is easy to discern. We note that there is also the possibility of small amounts of ROESY transfer, although we have yet to observe any discernible cross peaks with mixing times of 200 ms total, under the conditions of the experiment, with small sugar molecules.

The pulse sequence timing diagram for the 2D HEHAHA correlation spectrum is shown in Fig. 4 while Fig. 5 is the corresponding selective implementation of the experiment. The schematic

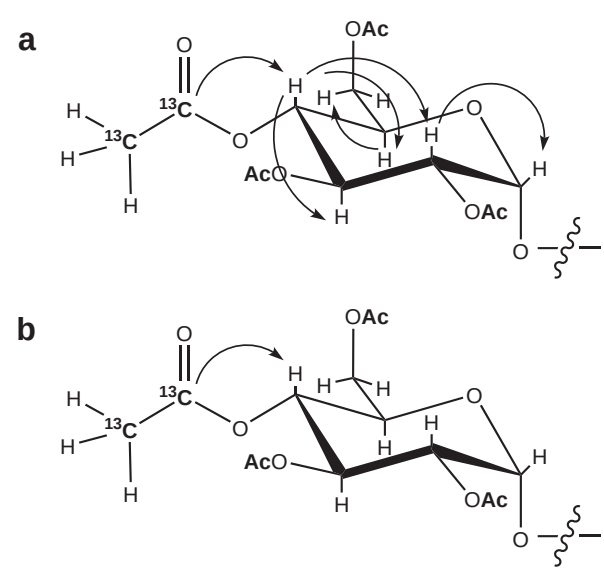

Fig. 6. Magnetization transfers occur during the (a) HEHAHA and (b) SHEHAHA pulse sequences. HEHAHA using DIPSI-2 results in transfer from the isotag carbonyl to many protons on the same sugar ring, while SHEHAHA limits the transfer almost exclusively to the proximal ring proton to the isotag.

magnetization transfers observed in maltitol with these two pulse sequences are laid out in Fig. 6.

Fig. 7 shows a comparison of the HEHAHA and SHEHAHA experiments carried out on a $CDCl_3$ solution of peracetylated maltitol. The top contour plot of Fig. 7 is the HEHAHA spectrum obtained using a simultaneous DIPSI-2 mixing sequence applied for 200 ms with a 930 Hz rf field strength. The proton and carbon transmitters were set in the center of the $^1H_{Ring}$ and ^{13}CO spectral ranges, respectively. Each acetyl ^{13}CO shows correlations to almost all $^1H_{Ring}$ in the same sugar ring as a result of simultaneous heteronuclear and homonuclear Hartmann–Hahn transfers. The protons (H4 and H1′) that lack a proximal labeled acetyl group, nevertheless show correlations to other acetyl groups in the spectrum. For larger oligosaccharides, these redundant correlation peaks result in crowded spectra and, when the digital resolution is limited in the indirect dimension, low-resolution spectra. In the SHEHAHA spectrum (7b) the redundant correlation peaks caused by homonuclear Hartmann–Hahn transfer are essentially eliminated. In both spectra, correlation peaks are inphase and absorptive; however, while HEHAHA requires additional *z*-filter elements [33] to eliminate the antiphase proton–proton terms, SHEHAHA inherently does not, as the offending homonuclear zero-quantum operators are never produced.

An alternative way to establish $^{13}CO - {}^1H_{Ring}$ correlations through three-bond J coupling is to use long-range INEPT-type coherence transfer, in which case there is no possibility of significant relayed magnetization transfer. On a practical level, the long-range INEPT coherence transfer avoids the technical difficulties of Hartmann–Hahn matching in the heteronuclear experiment and has superior sensitivity under comparable conditions. However, several factors may weigh against long-range INEPT with such small couplings.Cross peaks are antiphase with respect to the long-range heteronuclear coupling so no carbonyl decoupling can be used. Refocused long-range INEPT results in phase-modulated multiplets from the much larger $^{2,3}J_{HH}$ couplings which are much less useful for determining proton–proton coupling constants. As an example, a $^{13}CO - {}^1H_{Ring}$ constant-time heteronuclear correlation spectrum was recorded on the peracetylated maltitol sample using the pulse sequence in Fig. 8. A sample trace taken from the SHEHAHA spectrum (Fig. 7b) and constant time 2D heteronuclear correlation spectrum (data not shown) at the resonance frequency of carbon, C1, is shown in Fig. 9. The in-phase cross peaks in the SHEHAHA spectrum offer familiar multiplet structure, and are clearer and more compact than the antiphase cross peaks (Fig. 9b). While the SHEHAHA sensitivity is inferior to simple long-range INEPT, using a refocusing delay and *z*-filter to try to ob-

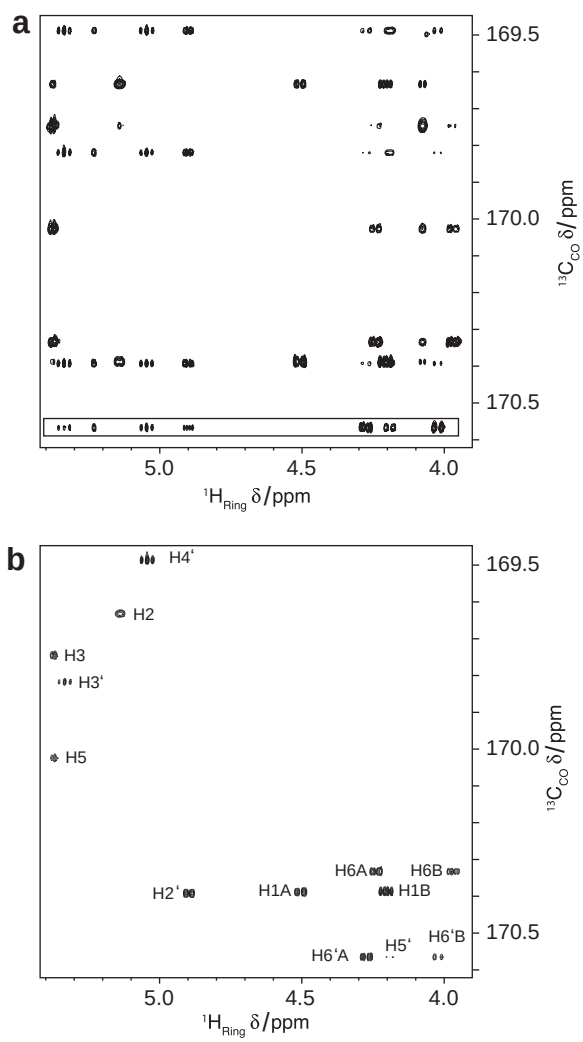

Fig. 7. Acetyl ^{13}CO and $^1H_{Ring}$ correlation spectra obtain using with (a) the HEHAHA sequence and (b) the SHEHAHA sequence. The two pulse sequences are laid out in Figs. 4 and 5. In both cases, data were acquired with 128 and 1500 complex data points over spectral widths of 300 and 3300 Hz in F_1 and F_2, respectively. Eight transients were recorded for each FID to give a total acquisition time of ~ 4 h for each spectrum. Data were processed by using nmrPipe/nmrDraw software. A simple cosine apodization function was applied in both t_1 and t_2 prior to 2D Fourier transformation. The boxed region in (a) shows protons correlated with a particular carbonyl isotag chemical shift. In (b) the assignments are shown. The weak peaks appearing at the chemical shift of H5′ result from residual unwanted TOCSY transfer between the H6′ protons and H5′, which has a chemical shift close to H6′A and is also coupled to it.

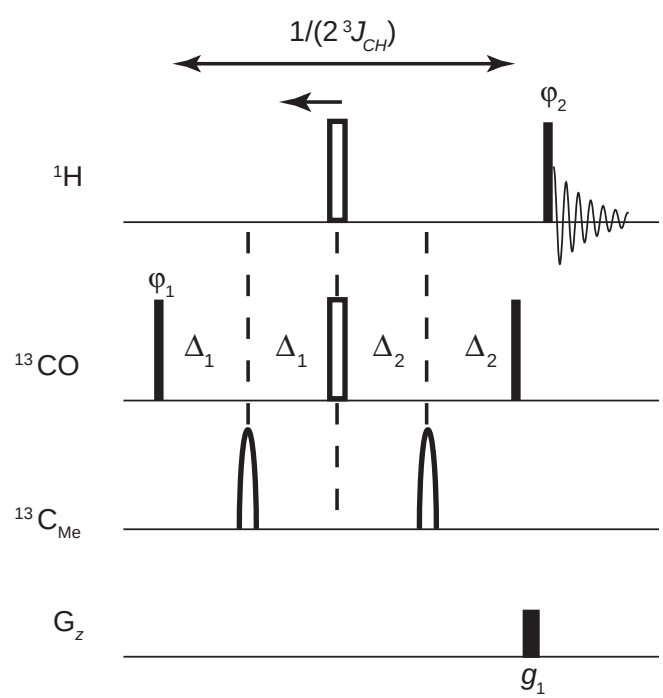

Fig. 8. Pulse sequence timing diagram for the constant-time reverse INEPT sequence. The constant time is set to optimize a representative long-range coupling, and chemical shift encoding is accomplished in the usual constant-time manner. The ^1H transmitter is set at the center of the ring proton region (4.7 ppm) and the ^{13}C transmitter is set at the center of the ^{13}CO region (170.0 ppm). $\Delta_1 = \left(\frac{J_{CH}}{8} - \frac{t_1}{4}\right), \Delta_2 = \left(\frac{J_{CH}}{8} + \frac{t_2}{4}\right)$, where J_{CH} is the $^{13}CO - {}^1H_{Ring}$ coupling constant. The phase cycle is $\varphi_1 = 4(x), 4(-x), \varphi_2 = (x, y, -x, -y)$, rec $= (x, y, -x, -y, -x, -y, x, y)$. Duration and strength of the gradient is, $g_1 = (900\ \mu s, 4.5\ G/cm)$.

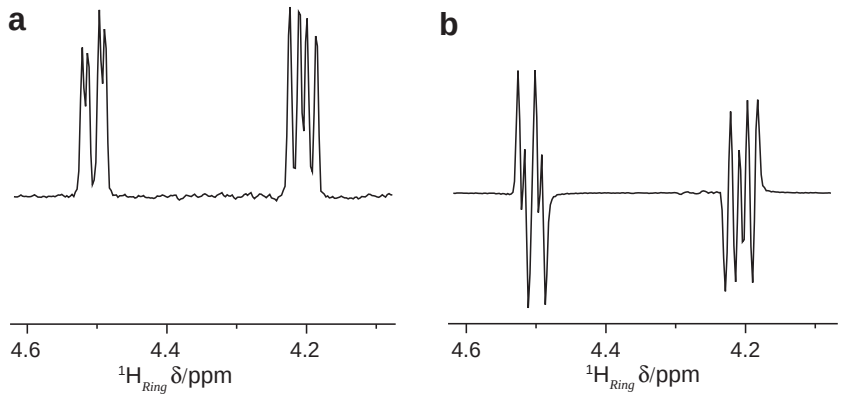

Fig. 9. Traces extracted from the 2D SHEHAHA (a) and 2D CT-HSQC (b) spectra, at the frequency of C1. The in-phase multiplet structure is more convenient, particularly if lines are somewhat broadened, or the heteronuclear coupling is small. Refocused INEPT yields phase-modulated multiplets, and after a *z*-filter to obtain an absorption in-phase structure, the sensitivity of the long-range INEPT experiment is inferior to SHEHAHA in most cases with acetylated sugars (data not shown).

tain *in-phase* proton multiplets results in sensitivity for the INEPT-based experiment that is worse than SHEHAHA for most cases, that depends on the particular proton–proton couplings in a complex way that is difficult to optimize, and that varies greatly from site to site. As the in-phase multiplets are essential for follow-on experiments like ROESY, to establish connectivity and/or branching of the sugars, SHEHAHA has a practically important role as a pulse sequence building block in these systems.

5. Conclusions

The SHEHAHA pulse sequence facilitates the structure elucidation of oligosaccharides that have been peracetylated with carbon-13 labeled acetyl groups. The method has been applied to peracetylated maltitol. Compared to HEHAHA and INEPT-type pulse scheme to correlate ^{13}CO and $^1H_{Ring}$ chemical shifts through the small three-bond J couplings, SHEHAHA shows the following advantages: (1) broadband heteronuclear Hartmann–Hahn transfer; (2) suppression of unwanted homonuclear Hartmann–Hahn transfer; (3) peaks are intrinsically in-phase and purely absorptive, so that no additional *z*-filter elements [33] are needed to eliminate the antiphase terms. Selective schemes to transfer in-phase magnetization using very moderate rf fields to highlight a few desired correlations can be an attractive alternative to 2D methods that may require carbon-13 decoupling across a wide bandwidth, as the decoupling of a localized region can be accomplished with far less power, and long proton acquisition times can be employed without damaging the probe or overheating the sample. We will report on these related experiments in the near future.

References

[1] S.R. Hartmann, E.L. Hahn, Nuclear double resonance in the rotating frame, Phys. Rev. 128 (1973) 2042–2053.
[2] A. Pines, M.G. Gibby, J.S. Waugh, Proton-enhanced NMR of dilute spins in solids, J. Chem. Phys. 59 (1962) 569–590.
[3] M.H. Levitt, R. Freeman, T. Frenkiel, Broad-band heteronuclear decoupling, J. Magn. Reson. 47 (1982) 328–330.
[4] A.J. Shaka, J. Keeler, T. Frenkiel, R. Freeman, An improved sequence for broad-band decoupling – WALTZ-16, J. Magn. Reson. 52 (1983) 335–338.
[5] A. Bax, D.G. Davis, MLEV-17-based two-dimensional homonuclear magnetization transfer spectroscopy, J. Magn. Reson. 65 (1985) 355–360.
[6] M. Rance, Improved techniques for homonuclear rotating-frame and isotropic mixing experiments, J. Magn. Reson. 74 (1987) 557–564.
[7] A.J. Shaka, C.J. Lee, A. Pines, Iterative schemes for bilinear operators – application to spin decoupling, J. Magn. Reson. 77 (1988) 274–293.
[8] S.P. Rucker, A.J. Shaka, Broadband homonuclear cross polarization in 2D NMR using DIPSI-2, Mol. Phys. 68 (1989) 509–517.
[9] L. Braunschweiler, R.R. Ernst, Coherence transfer by isotropic mixing – application to proton correlation spectroscopy, J. Magn. Reson. 53 (1983) 521–528.
[10] A. Mohebbi, A.J. Shaka, Improvements in C-13 broad-band homonuclear cross-polarization for 2D and 3D NMR, Chem. Phys. Lett. 178 (1991) 374–378.
[11] L.R. Brown, B.C. Sanctuary, Hetero-TOCSY experiments with WALTZ and DIPSI mixing sequences, J. Magn. Reson. 91 (1991) 413–421.
[12] J.M. Richardson, R.T. Clowes, W. Boucher, P.J. Domaille, C.H. Hardman, J. Keeler, E.D. Laue, The use of heteronuclear cross polarization to enhance the sensitivity of triple-resonance NMR experiments – improved 4D HCNNH pulse sequences, J. Magn. Reson. Ser. B 101 (1993) 223–227.
[13] T. Carlomagno, B. Luy, S.J. Glaser, "Kin" HEHAHA sequences, heteronuclear Hartmann–Hahn transfer with different bandwidths for spins I and S, J. Magn. Reson. 126 (1997) 110–119.
[14] E.R.P. Zuiderweg, L. Zeng, B. Brutscher, R.C. Morshauser, Band-selective hetero- and homonuclear cross-polarization using trains of shaped pulses, J. Biomol. NMR 8 (1996) 147–160.
[15] B. Bendiak, T.T. Fang, D.N.M. Jones, An effective strategy for structural elucidation of oligosaccharides through NMR spectroscopy combined with peracetylation using doubly C-13-labeled acetyl groups, Can. J. Chem. 80 (2002) 1032–1050.
[16] D.N.M. Jones, B. Bendiak, Novel multi-dimensional heteronuclear NMR techniques for the study of ^{13}C-*O*-acetylated oligosaccharides: expanding the dimensions for carbohydrate structures, J. Biomol. NMR 15 (1999) 157–168.
[17] G.S. Armstrong, V.A. Mandelshtam, A.J. Shaka, B. Bendiak, Rapid high-resolution four-dimensional NMR spectroscopy using the filter diagonalization method and its advantages for detailed structural elucidation of oligosaccharides, J. Magn. Reson. 173 (2005) 160–168.
[18] G.A. Morris, R. Freeman, Enhancement of nuclear magnetic resonance signals by polarization transfer, J. Am. Chem. Soc. 101 (1979) 760–762.
[19] A. Bax, M.F. Summers, H-1 and C-13 assignments from sensitivity-enhanced detection of heteronuclear multiple-bond connectivity by 2D multiple quantum NMR, J. Am. Chem. Soc. 108 (1986) 2093–2094.
[20] A. Bax, D.G. Davis, S.K. Sarkar, An improved method for two-dimensional heteronuclear relayed-coherence-transfer NMR spectroscopy, J. Magn. Reson. 63 (1985) 230–234.
[21] L. Müller, R.R. Ernst, Coherence transfer in the rotating frame, application to heteronuclear cross-correlation spectroscopy, Mol. Phys. 38 (1979) 963–992.
[22] G.C. Chingas, A.N. Garroway, R.D. Bertrand, W.B. Moniz, Zero quantum NMR in the rotating frame – J-cross polarization in AX_n systems, J. Chem. Phys. 74 (1981) 127–156.
[23] M. Ernst, C. Griesinger, R.R. Ernst, W. Bermel, Optimized heteronuclear cross polarization in liquids, Mol. Phys. 74 (1991) 219–252.
[24] U. Haeberlen, J.S. Waugh, Coherent averaging effects in magnetic resonance, Phys. Rev. 175 (1968) 453–467.
[25] M.L. Remeroski, S.J. Glaser, G.P. Drobny, A theoretical-study of coherence transfer by isotropic mixing – calculation of pulse sequence performance for systems of biological interest, J. Magn. Reson. 68 (1989) 110–131.
[26] J. Cavanagh, W.J. Chazin, M. Rance, The time dependence of coherence transfer in homonuclear isotropic mixing experiments, J. Magn. Reson. 87 (1990) 110–131.
[27] J. Schleucher, J. Quant, S.J. Glaser, C. Griesinger, A theorem relating cross-relaxation and Hartmann–Hahn transfer in multiple-pulse sequences – optimal suppression of TOCSY transfer in ROESY, J. Magn. Reson. A 112 (1995) 144–151.
[28] J. Keeler, D. Neuhaus, False transverse NOE enhancements in CAMELSPIN spectra, J. Magn. Reson. 68 (1986) 568–574.
[29] K. Ishihara, M. Kubota, H. Kurihara, H. Yamamoto, Scandium trifluoromethanesulfonate as an extremely active Lewis acid catalyst in

acylation of alcohols with acid anhydrides and mixed anhydrides, J. Org. Chem. 61 (1996) 4560–4567.
[30] A.J. Shaka, J. Keeler, Broadband spin decoupling in isotropic liquids, Prog. NMR Spect. 19 (1987) 47–129.
[31] M.J. Thrippleton, J. Keeler, Elimination of zero-quantum interference in two-dimensional NMR spectra, Angew. Chem. Int. Ed. 42 (2003) 3938–3941.
[32] D. Marion, M. Ikura, R. Tschudin, A. Bax, Rapid recording of 2D NMR spectra without phase cycling – application to the study of hydrogen-exchange in proteins, J. Magn. Reson. 85 (1989) 393–399.
[33] O.W. Sørensen, M. Rance, R.R. Ernst, *z*-filters for purging phase-distorted or multiplet-distorted spectra, J. Magn. Reson. 56 (1984) 527–534.